Supplementary Information (SI) for Chemical Science.
This journal is © The Royal Society of Chemistry 2026

Electronic Supplementary Information (ESI)

Nanoscale Ru unlocking nanoneedles assembled hierarchical CoO microspheres toward efficient nitrate-to-ammonia electroconversion

Jinxiu Zhao,[a] Xuejing Liu,[b] Xiang Ren,[b,] Dan Zhao,[b] Zhen Li,[b] Qing Kang,[b] Chang-wen Zhang,[c] Linrui Hou,[a] Qin Wei,[b,]* and Changzhou Yuan[a,]**

[a] School of Material Science & Engineering, University of Jinan, Jinan, 250022, P. R. China

E-mail: mse_yuancz@ujn.edu.cn; ayuancz@163.com (*Prof.* C. Yuan)

[b] Collaborative Innovation Centre for Green Chemical Manufacturing and Accurate Detection, School of Chemistry and Chemical Engineering, University of Jinan, Jinan, 250022, P. R. China

E-mail: chem_renx@163.com (*Prof.* X. Ren); sdjndxwq@163.com (*Prof.* Q. Wei)

[c] School of Physics and Technology, University of Jinan, Jinan, 250022, P. R. China

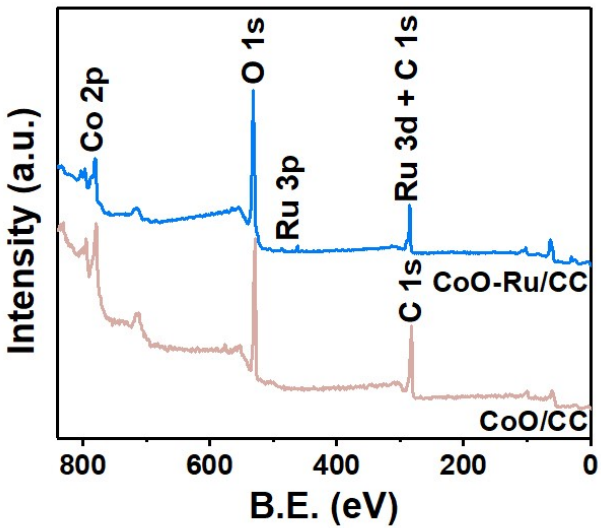

Fig. S1. XPS survey spectra of CoO/CC and CoO-Ru/CC.

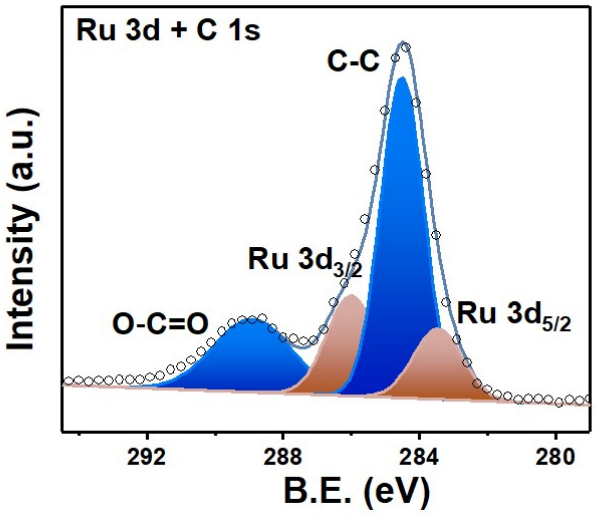

Fig. S2. XPS spectra of CoO-Ru/CC in the Ru 3d and C 1s core level.

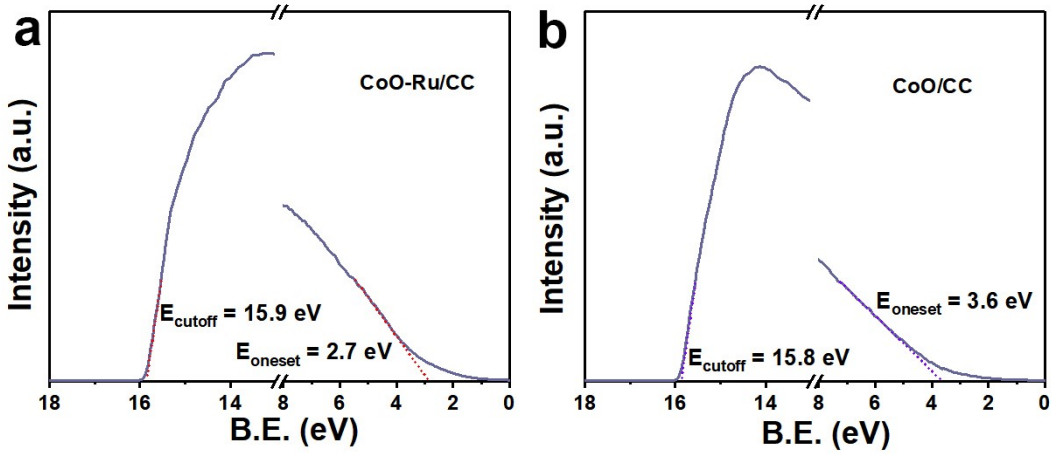

Fig. S3. Typical UPS spectra of (a) CoO-Ru/CC and (b) CoO/CC.

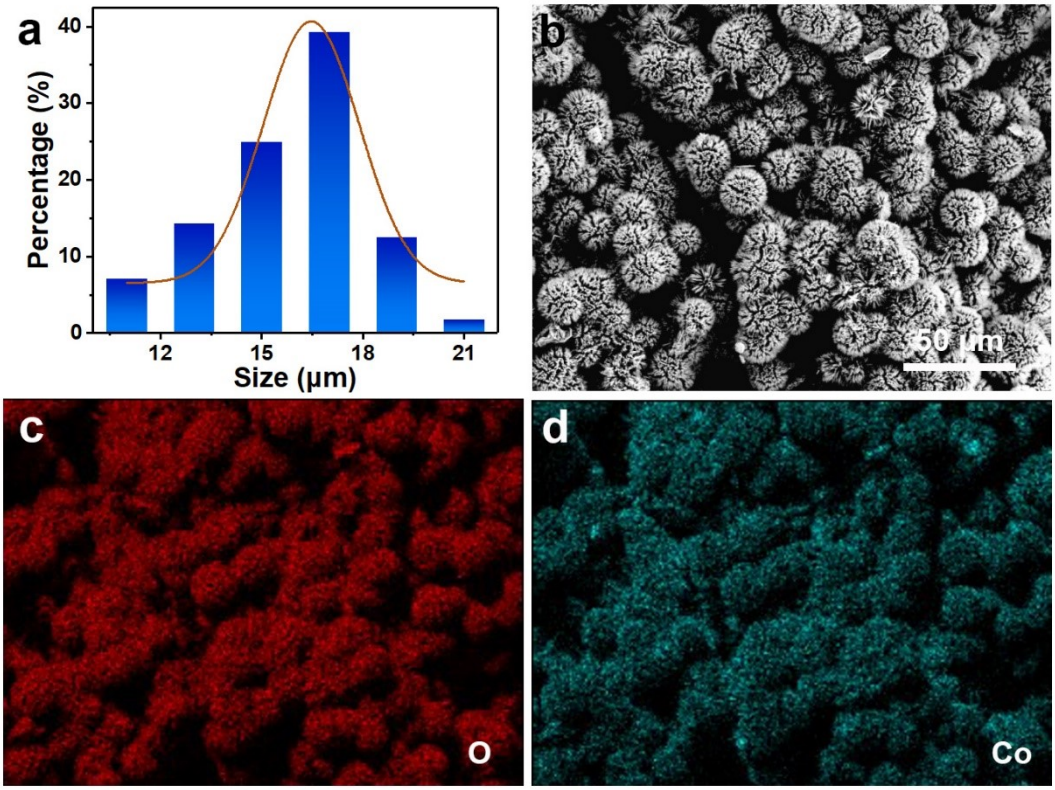

Fig. S4. (a) Size distribution diagram of CoO MSs. (b-d) FESEM and corresponding EDX elemental mapping images of CoO MSs.

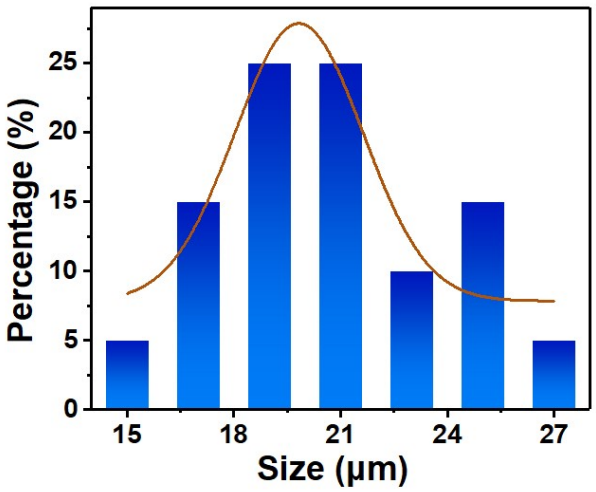

Fig. S5. Size distribution diagram of CoO-Ru MSs.

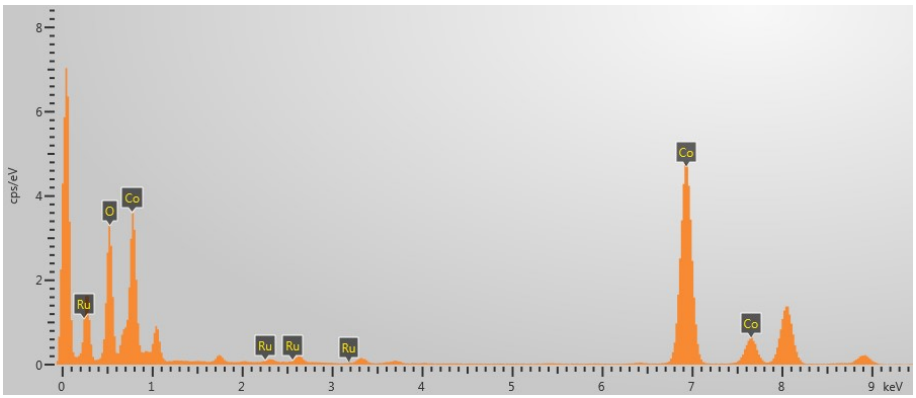

Fig. S6. EDX spectrum of CoO-Ru.

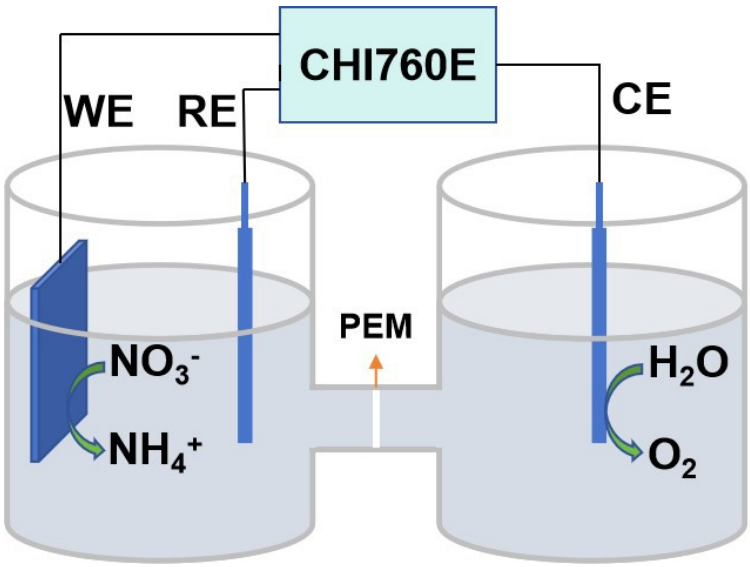

Fig. S7. H-type electrocatalytic cell for $eRNO_3^-$-to-NH_3.

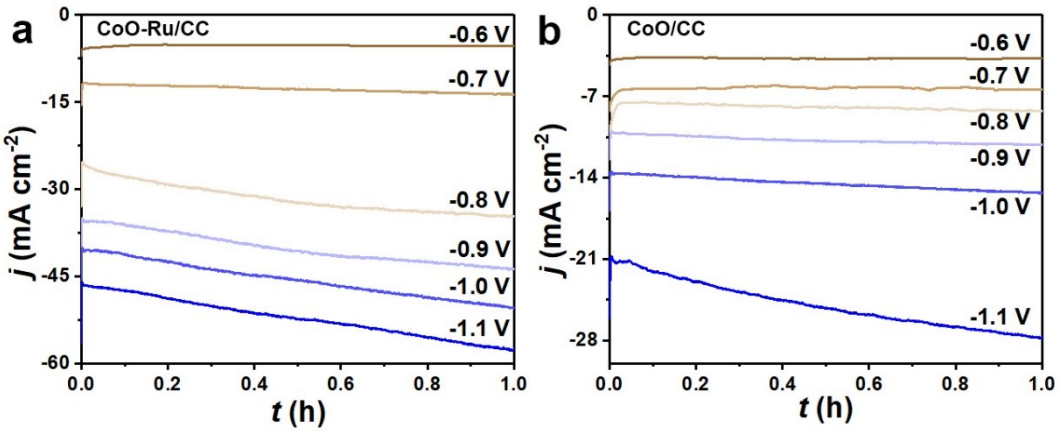

Fig. S8. *j-t* curves of (a) CoO-Ru/CC and (b) CoO/CC at series of potentials in 0.1 M Na_2SO_4 with 0.01 M $NaNO_3$ electrolyte.

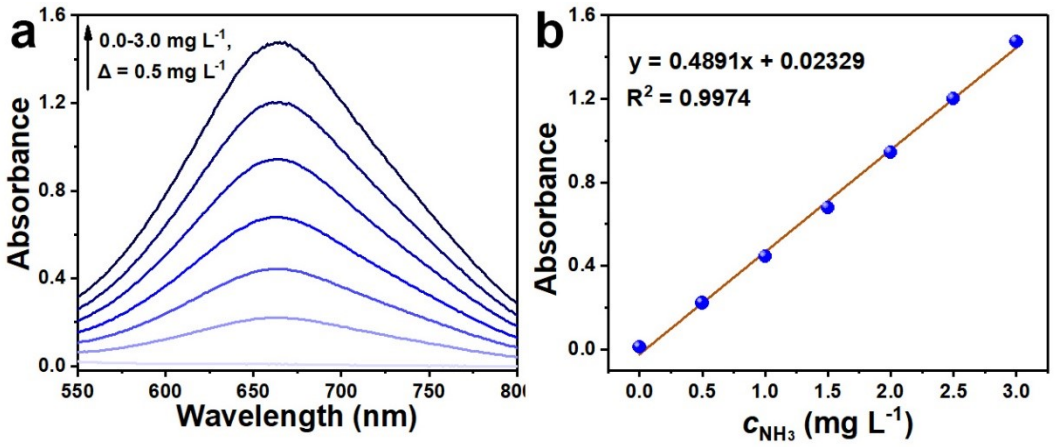

Fig. S9. (a) UV−Vis spectra of various NH_3 concentrations. (b) Calibration curve used to calculate NH_3 concentration.

The Indophenol Blue spectrophotometric method for determining NH_3 as follows. Firstly, 50 μL of oxidizing agent (NaClO) and 0.75 M NaOH, 500 μL of coloring agent (0.4 M $C_7H_5O_3Na$ and 0.32 M NaOH), and 50 μL of catalyst (1.0 wt% $Na_2[Fe(CN)_5NO]\cdot H_2O$) were added into the diluted electrolyte (4 mL) from the cathodic cell accordingly and mixed uniformly. After standing at 25 °C for 2 h, the ultraviolet and visible (UV-Vis) absorption spectrum was measured. The concentration of indophenol blue was determined using the absorbance at a wavelength of 660 nm.

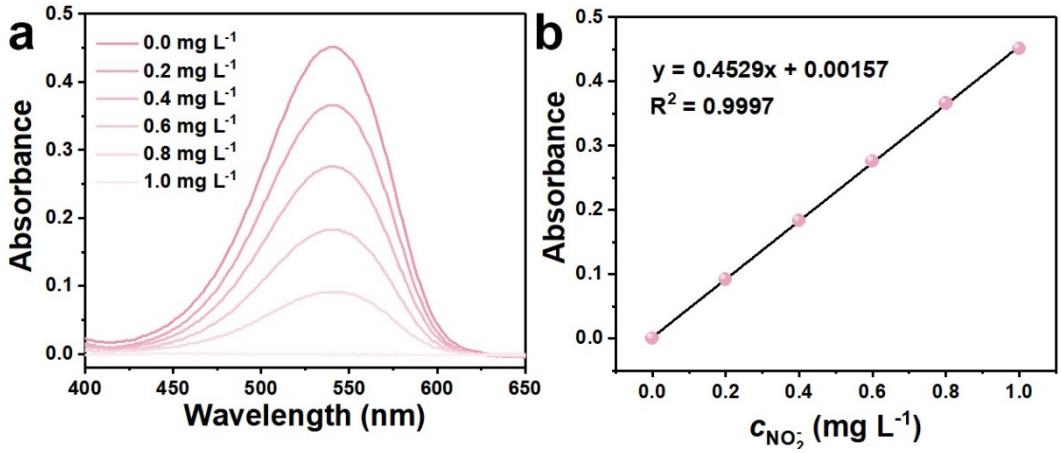

Fig. S10. (a) UV−Vis spectra of various NH_3 concentrations. (b) Calibration curve used to calculate NO_2^- concentration.

The chromogenic agent of NO_2^- contains 4 g $C_6H_4SO_2N_2H_4$, 0.2 g $C_{12}H_{16}Cl_2N_2$, 10 mL H_3PO_4 (ρ = 1.70 g mL^{-1}), and 50 mL H_2O. Firstly, a certain amount of electrolyte was taken from the cathodic cell with a pipette gun and diluted it to 5 mL. Then, 100 μL of chromogenic agent was added into the diluted electrolyte and mixed uniformly. The absorbance intensity of the aforementioned solution after kept for 25 min was recorded at the wavelengths of 540 nm. The related concentration-absorbance curve was recorded from a series of known standard concentration of $NaNO_2$ solutions and the fitted curve is y = 0.04529x + 0.00157, R^2 = 0.9997.

The $FE_{NO_2^-}$ were calculated using the following equation:

$$FE_{NO_2^-} = \frac{2 \times F \times c_{NO_2^-} \times V}{46 \times 10^6 \times Q} \times 100\%$$

where $c_{NO_2^-}$ (mg L^{-1}), V (L), t (h), A (cm^2), F and Q (C) were the measured NO_2^- concentration, electrolyte volume, reaction time, the geometric area of the catalyst, Faraday constant (96485 C mol^{-1}), and quantity of electric charge, respectively.

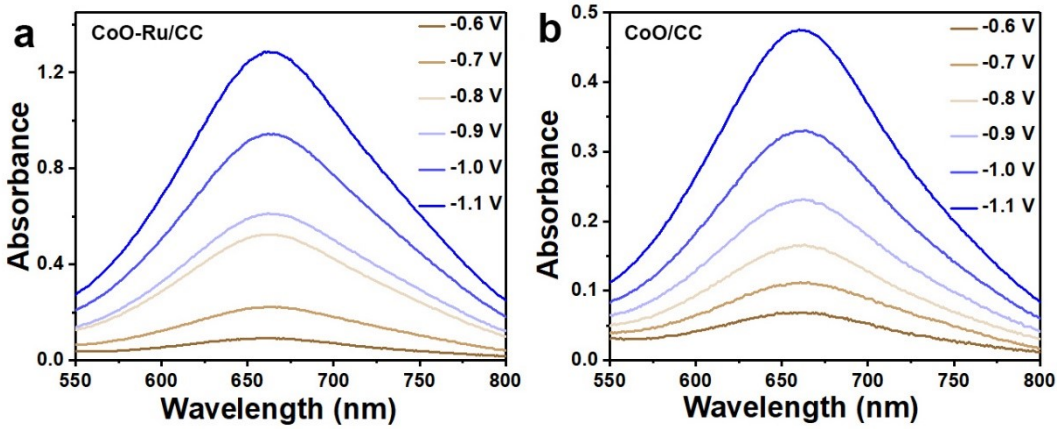

Fig. S11. UV-Vis spectra of electrolytes after 1-h catalytic action by (a) CoO-Ru/CC and (b) CoO/CC (dilute 150 μL of electrolyte to 4 mL).

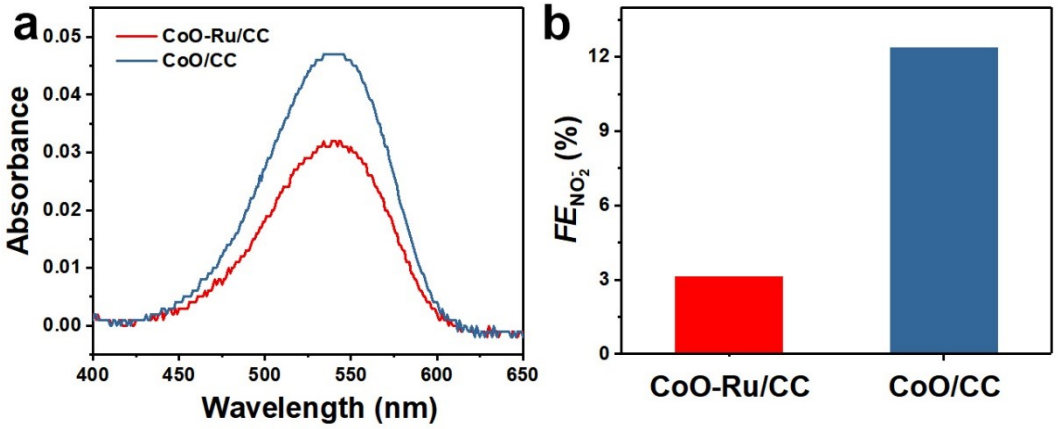

Fig. S12. (a) UV spectra and (b) $FE_{NO_2^-}$ of CoO-Ru/CC and CoO/CC.

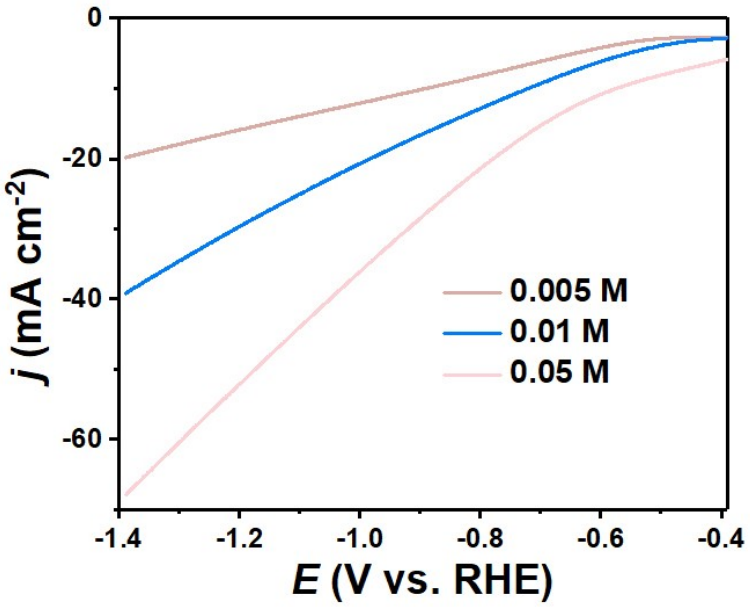

Fig. S13. LSV curves of CoO-Ru/CC in 0.1 M Na_2SO_4 with series of $NaNO_3$ electrolytes.

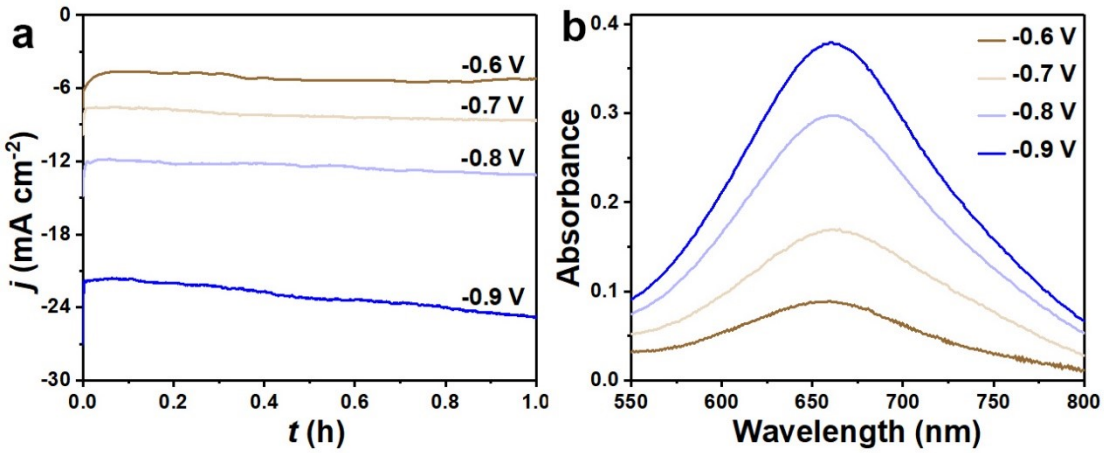

Fig. S14. (a) *j-t* curves of CoO-Ru/CC at series of potentials in 0.1 M Na_2SO_4 with 0.005 M $NaNO_3$ electrolyte. (b) UV-Vis spectra of electrolytes that dilute 150 μL of electrolyte to 4 mL.

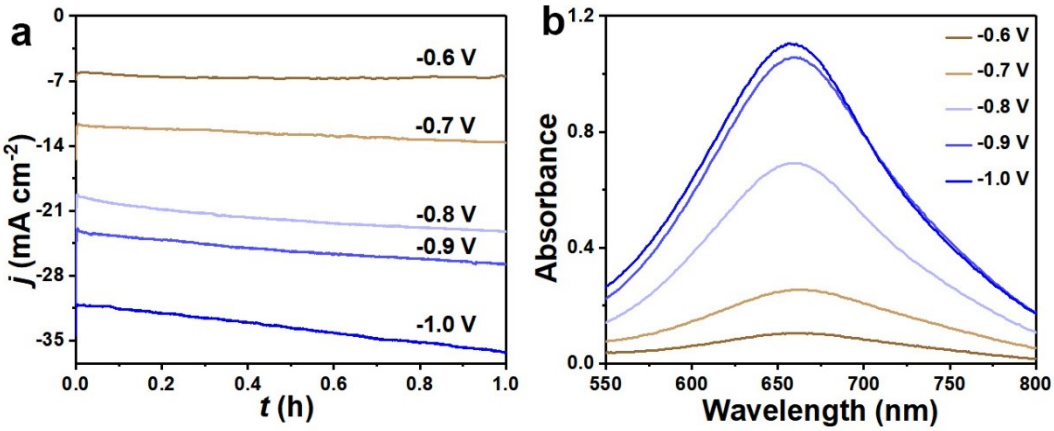

Fig. S15. (a) *j-t* curves of CoO-Ru/CC at series of potentials in 0.1 M Na_2SO_4 with 0.05 M $NaNO_3$ electrolyte. (b) UV-Vis spectra of electrolytes that dilute 150 μL of electrolyte to 4 mL.

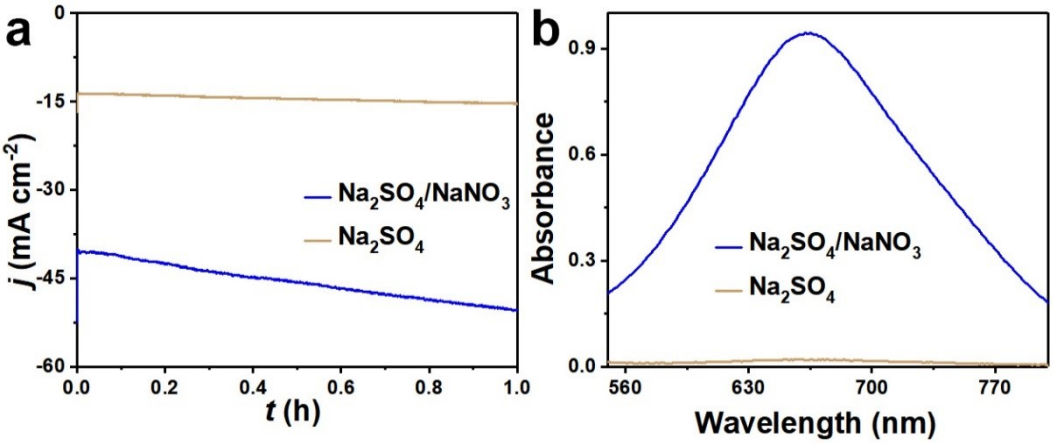

Fig. S16. (a) *j-t* curves of CoO-Ru/CC at −1.0 V *vs.* RHE in 0.1 M Na_2SO_4 with or without 0.01 M $NaNO_3$ electrolyte. (b) UV-Vis spectra of electrolytes that dilute 150 μL of electrolyte to 4 mL.

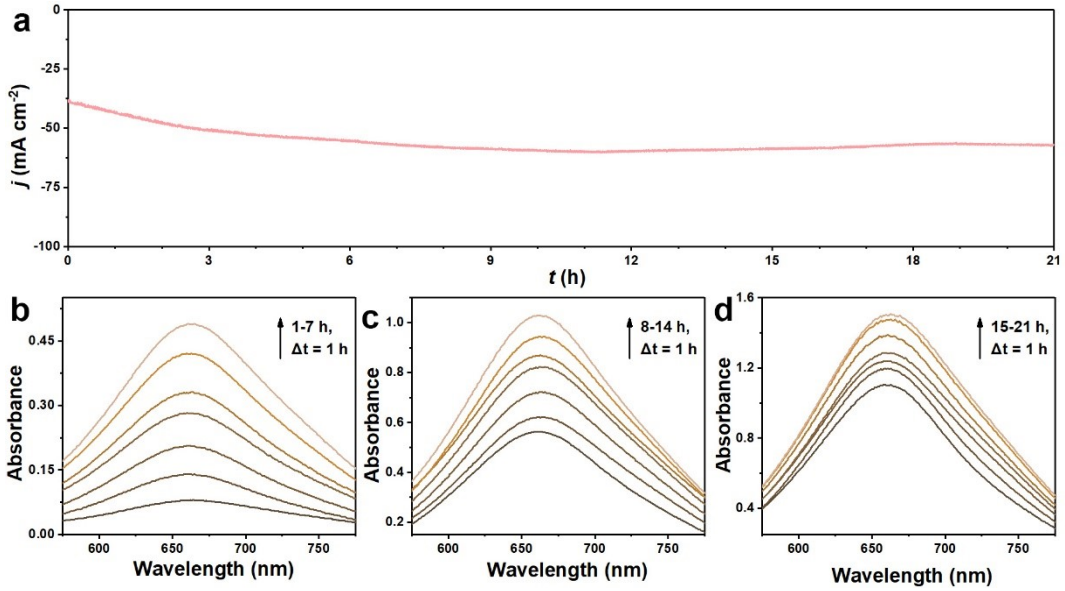

Fig. S17. (a) Long-time *j-t* curve of CoO-Ru/CC for 21-h NO_3^- reduction experiment at −1.0 V *vs.* RHE in 0.1 M Na_2SO_4 with 0.05 M $NaNO_3$ electrolyte. (b-d) UV-Vis spectra of electrolytes that dilute 30 μL of electrolyte to 4 mL.

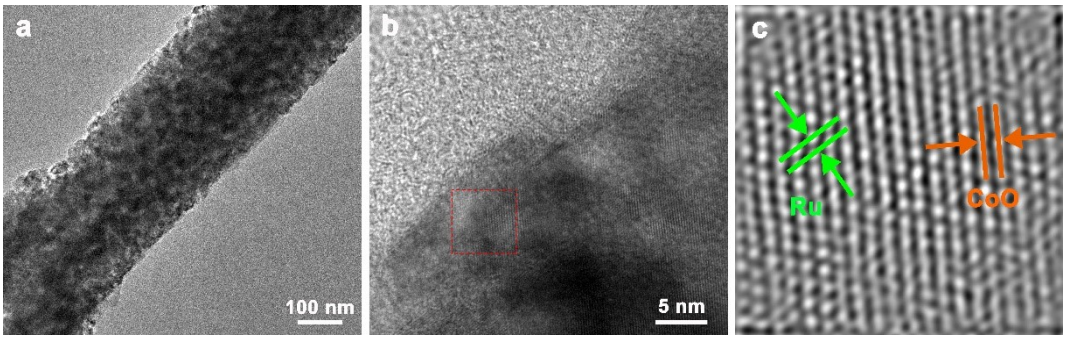

Fig. S18. (a) TEM, (b) HRTEM and (c) corresponding IFFT images from red dotted region in (b) of CoO-Ru after NO_3^- reduction experiment.

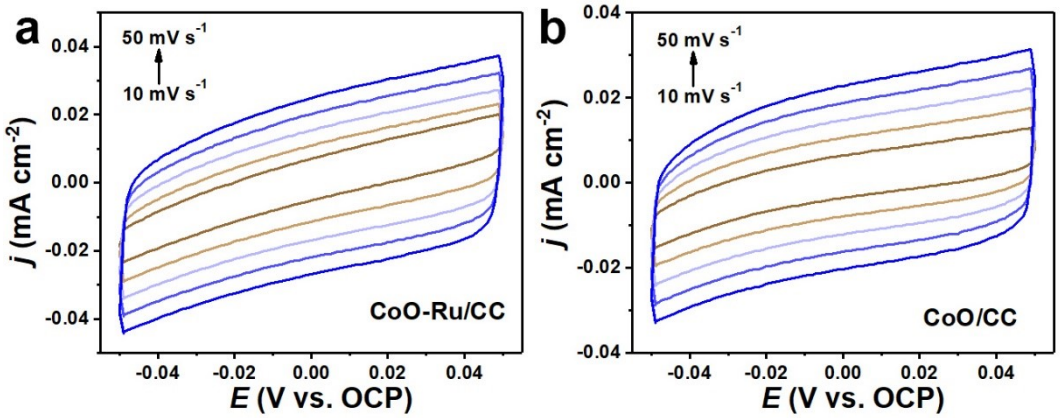

Fig. S19. The cyclic voltammograms at different scan rates (10, 20, 30, 40, and 50 mV s^{-1}) for (a) CoO-Ru/CC and (b) CoO/CC.

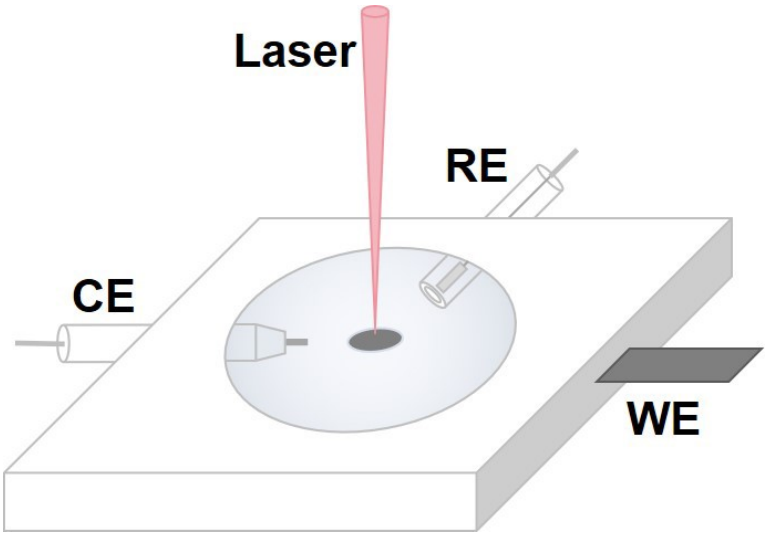

Fig. S20. Schematic diagram of in-situ Raman device.

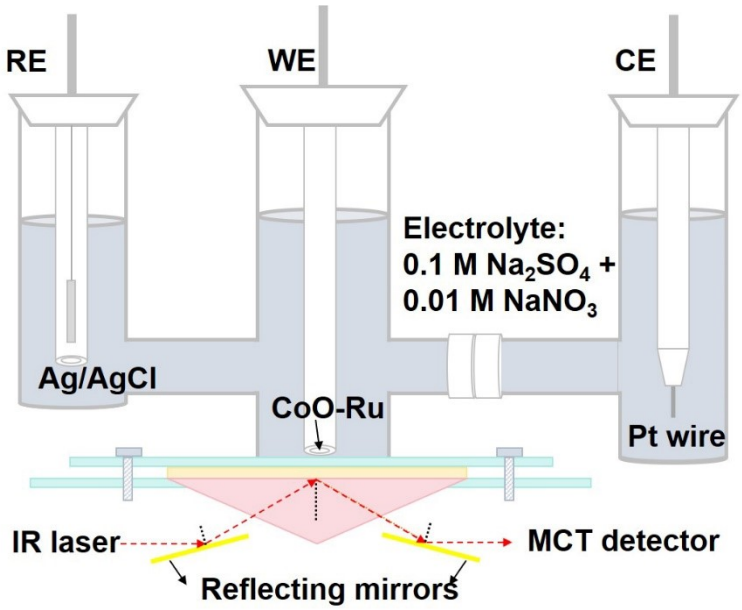

Fig. S21. Schematic diagram of in-situ ATR-FTIR device.

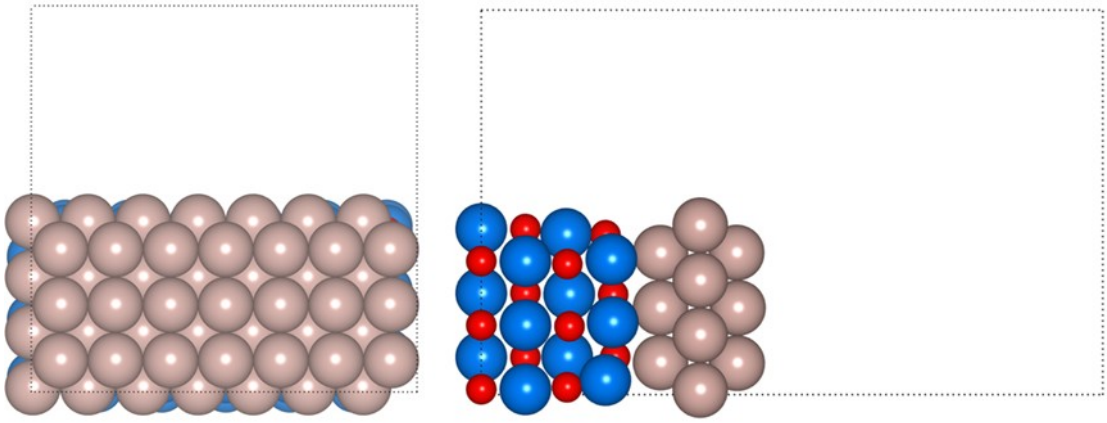

Fig. S22. Schematic diagram of the CoO-Ru interfacial structure. (top and side views). The O, Co and Ru atoms are shown in red, blue and pale brown colors, respectively.

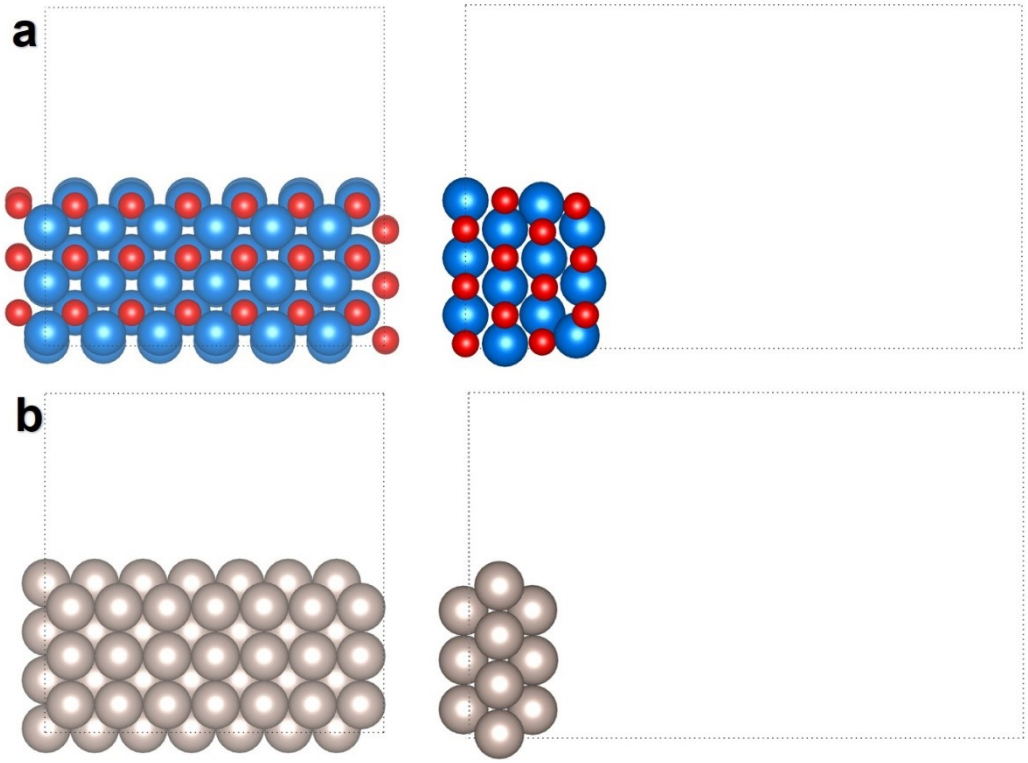

Fig. S23. Schematic diagram of the (a) CoO and (b) Ru interfacial structure. (top and side views). The O, Co and Ru atoms are shown in red, blue and pale brown colors, respectively.

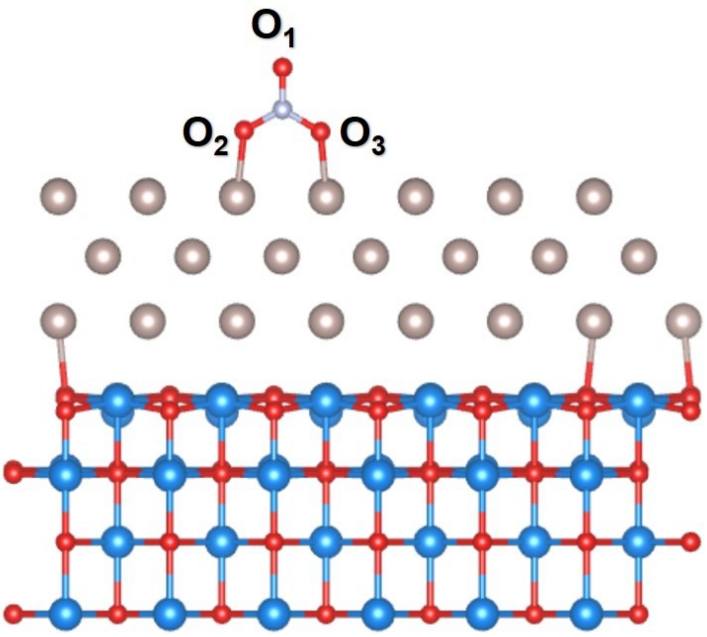

Fig. S24. Schematic diagram N−O bond lengths of NO_3^- species adsorbed on CoO-Ru.

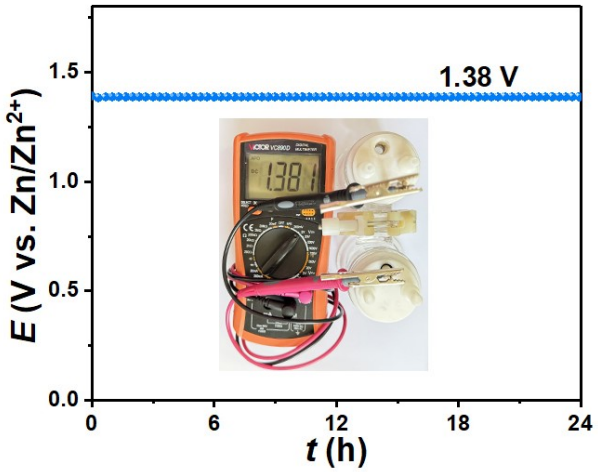

Fig. S25. OCP of CoO/CC based Zn-NO_3^- battery.

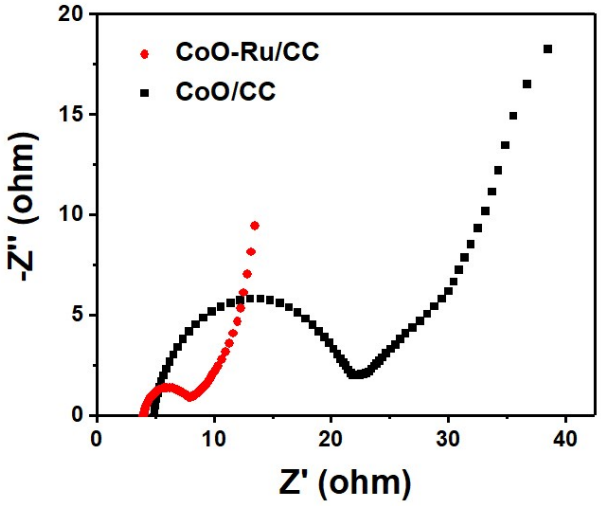

Fig. S26. Nyquist plots of CoO-Ru/CC and CoO/CC.

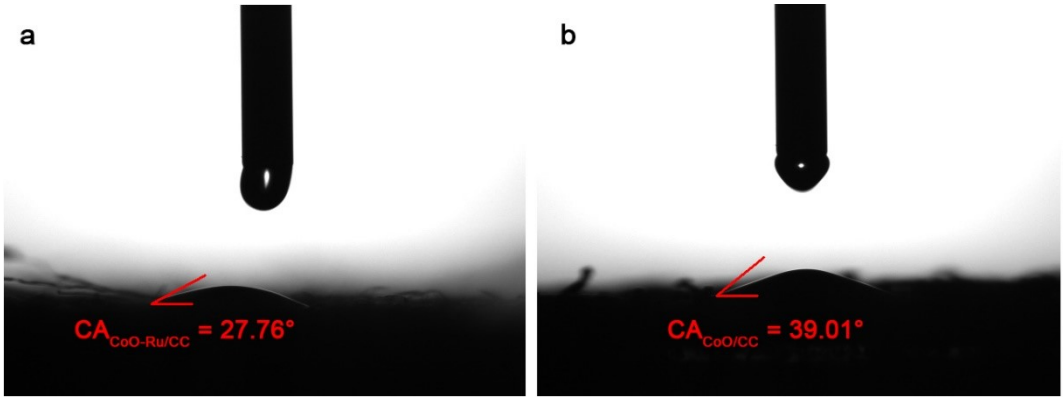

Fig. S27. Contact angle photos for of (a) CoO-Ru/CC and (b) CoO/CC.

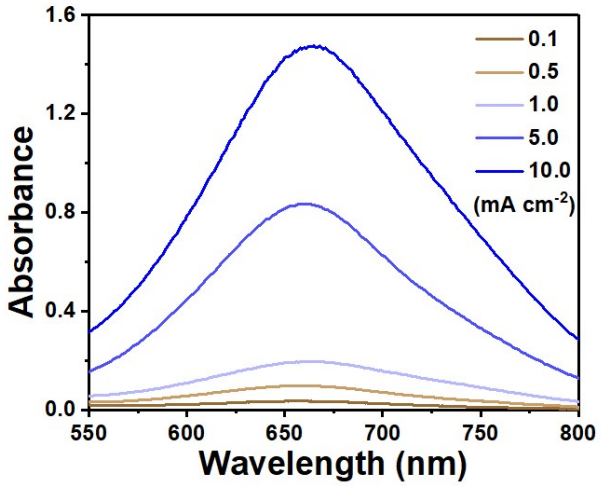

Fig. S26. UV-Vis spectra of electrolytes after one hour of discharge at various discharge current densities.

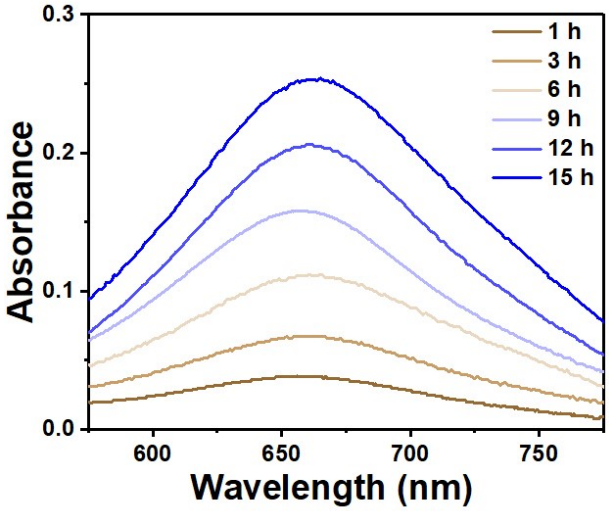

Fig. S27. UV-Vis spectra of electrolytes at time-series points in 15-h long-term discharging test.

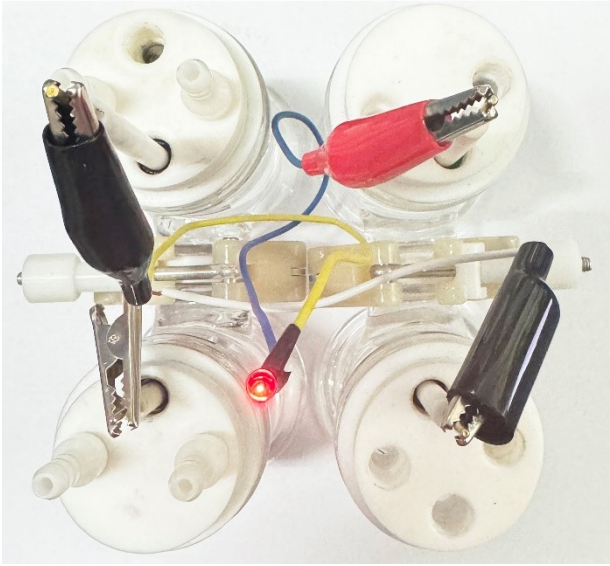

Fig. S28. Digital photos for powering a LED by two CoO-Ru/CC based Zn−NO_3^- batteries connected in series.

Table S1. Comparison of the NH_3 electrosynthesis activity for CoO-Ru/CC with other catalysts.

Catalyst	NH_3 yield rate ($mg\ h^{-1}\ cm^{-2}$)	FE (%)	Ref.
CoO-Ru/CC	2.502	93.41	This work
Au/C	0.442	26	1
Cu@C	0.476	72	2
Rh NFs	0.255	95	3
2Z-ZCO	2.04	90.2	4
NJUZ-2	1.564	91	5
BP/Nb_2C	0.595	90.3	6
Fe-MoS_2	0.306	98	7
Ag-Co_3O_4	0.884	88	8
CuCl_BEF	1.819	44.7	9
CuO NWAs	2.244	95.8	10
Au-NCs/PtTeAu-MLs	0.391	96.3	11
Pd-NDs/Zr-MOF	1.955	58.1	12
Cu/Co0.85SeVSe	2.363	93.5	13
PTCDA/o-Cu	0.442	77	14
Ru SA-NC	2.278	72.8	15
GdSA_D_NiO400	0.833	97	16
PdCuAg MTs	1.768	95.16	17
PdCuRu MSs	0.85	95	18
NTCDA-LIG	2.465	83.7	19

References

1 J. Choi, H.-L. Du, C. K. Nguyen, B. H. R. Suryanto, A. N. Simonov and D. R. Macfarlane, *ACS Energy Lett.*, 2020, **5**, 2095−2097.

2 Z. Song, Y. Liu, Y. Zhong, Q. Guo, J. Zeng and Z. Geng, *Adv. Mater.*, 2022, **34**, 2204306.

3 H. Liu, J. Timoshenko, L. Bai, Q. Li, M. Rüscher, C. Sun, B. R. Cuenya and J. Luo, *ACS Catal.*, 2023, **13**, 1513−1521.

4 S. Dong, A. Niu, K. Wang, P. Hu, H. Guo, S. Sun, Y. Luo, Q. Liu, X. Sun and T. Li, *Appl. Catal. B: Environ.*, 2023, **333**, 122772.

5 M. Wang, S. Li, Y. Gu, W. Xu, H. Wang, J. Sun, S. Chen, Z. Tie, J.-L. Zuo, J. Ma, J. Su and Z. Jin, *J. Am. Chem. Soc.*, 2024, **146**, 20439−20448.

6 S. Wang, C. Song, Y. Cai, Y. Li, P. Jiang, H. Li, B. Yu and T. Ma, *Adv. Energy Mater.*, 2023, **13**, 2301136.

7 J. Li, Y. Zhang, C. Liu, L. Zheng, E. Petit, K. Qi, Y. Zhang, H. Wu, W. Wang, A. Tiberj, X. Wang, M. Chhowalla, L. Lajaunie, R. Yu and D. Voiry, *Adv. Funct. Mater.*, 2022, **32**, 2108316.

8 M. Zhang, Z. Ma, S. Zhou, C. Han, V. Kundi, P. V. Kumar, L. Thomsen, B. Johannessen, L. Peng, Y. Shan, C. Tsounis, Y. Yang, J. Pan and R. Amal, *ACS Catal.*, 2024, **14**, 11231−11242.

9 W.-J. Sun, H.-Q. Ji, L.-X. Li, H.-Y. Zhang, Z.-K. Wang, J.-H. He and J.-M. Lu, *Angew. Chem., Int. Ed.*, 2021, **60**, 22933−22939.

10 Y. Wang, W. Zhou, R. Jia, Y. Yu and B. Zhang, *Angew. Chem., Int. Ed.*, 2020, **59**, 5350–5354.

11 Q.-L. Hong, B. Sun, X. Ai, X.-L. Tian, F.-M. Li and Y. Chen, *Adv. Funct. Mater.*, 2024, **34**, 2310730.

12 M. Jiang, J. Su, X. Song, P. Zhang, M. Zhu, L. Qin, Z. Tie, J.-L. Zuo and Z. Jin, *Nano Lett.*, 2022, **22**, 2529−2537.

13 Z. Gu, Y. Zhang, X. Wei, Z. Duan, Q. Gong and K. Luo, *Adv. Mater.*, 2023, **35**, 2303107.

14 G.-F. Chen, Y. Yuan, H. Jiang, S.-Y. Ren, L.-X. Ding, L. Ma, T. Wu, J. Lu and H. Wang, *Nat. Energy*, 2020, **5**, 605−613.

15 Z. Ke, D. He, X. Yan, W. Hu, N. Williams, H. Kang, X. Pan, J. Huang, J. Gu and X. Xiao, *ACS Nano*, 2023, **17**, 3483−3491.

16 A. Kumar, J. Lee, M. G. Kim, B. Debnath, X. Liu, Y. Hwang, Y. Wang, X. Shao, A. R. Jadhav, Y. Liu, H. Tüysüz and H. Lee, *ACS Nano*, 2022, **16**, 15297−15309.

17 L. Sun, H. Yao, Y. Wang, C. Zheng and B. Liu, *Adv. Energy Mater.*, 2023, **13**, 2303054.

18 L. Sun, H. Yao, F. Jia, Y. Wang and B. Liu, *Adv. Energy Mater.*, 2023, **13**, 2302274.

19 L. Cheng, T. Ma, B. Zhang, L. Huang, W. Guo, F. Hu, H. Zhu, Z. Wang, T. Zheng, D.-T. Yang, C.-K. Siu, Q. Liu, Y. Ren, C. Xia, B. Z. Tang and R. Ye, *ACS Catal.*, 2022, **12**, 11639−11650.